OXFORD

International Journal of Neuropsychopharmacology, (2016) 19(8): 1–13

doi:10.1093/injp/pyw035
Advance Access Publication: April 21, 2016
Research Article

RESEARCH ARTICLE

Valproic Acid and Other HDAC Inhibitors Upregulate FGF21 Gene Expression and Promote Process Elongation in Glia by Inhibiting HDAC2 and 3

Yan Leng, MD; Junyu Wang, BS; Zhifei Wang, PhD; Hsiao-Mei Liao, PhD; Monica Wei; Peter Leeds, BS; De-Maw Chuang, PhD

Molecular Neurobiology Section, National Institute of Mental Health, National Institutes of Health, Bethesda, MD.

Correspondence: De-Maw Chuang, PhD, Molecular Neurobiology Section, National Institute of Mental Health, National Institutes of Health, 10 Center Drive MSC 1363, Bethesda, MD 20892–1363 (chuang@mail.nih.gov); Yan Leng, MD, Molecular Neurobiology Section, National Institute of Mental Health, National Institutes of Health, 10 Center Drive MSC 1363, Bethesda, MD 20892–1363 (lengy@mail.nih.gov).

Abstract

Background: Fibroblast growth factor 21, a novel regulator of glucose and lipid metabolism, has robust protective properties in neurons. However, its expression and function in glia are unknown. Valproic acid, a mood stabilizer and anticonvulsant, is a histone deacetylase inhibitor and a dynamic gene regulator. We investigated whether histone deacetylase inhibition by valproic acid and other inhibitors upregulates fibroblast growth factor 21 expression and, if so, sought to identify the histone deacetylase isoform(s) involved and their role in altering glial cell morphology.
Methods: C6 glioma or primary cortical glial cultures were treated with histone deacetylase inhibitors, and fibroblast growth factor 21 levels and length of cell processes were subsequently measured. Histone deacetylase 1, 2, or 3 was also knocked down to detect which isoform was involved in regulating fibroblast growth factor 21 mRNA levels. Finally, knockdown and overexpression of fibroblast growth factor 21 were performed to determine whether it played a role in regulating cell process length.
Results: Treatment of C6 cells or primary glial cultures with valproic acid elevated fibroblast growth factor 21 mRNA levels, extended cell process length, and markedly increased acetylated histone-H3 levels. Other histone deacetylase inhibitors including pan- and class I-specific inhibitors, or selective knockdown of histone deacetylase 2 or 3 isoform produced similar effects. Knockdown or overexpression of fibroblast growth factor 21 significantly decreased or increased C6 cell process length, respectively.
Conclusions: In glial cell line and primary glia, using pharmacological inhibition and selective gene silencing of histone deacetylases to boost fibroblast growth factor 21 mRNA levels results in elongation of cell processes. Our study provides a new mechanism via which histone deacetylase 2 and 3 participate in upregulating fibroblast growth factor 21 transcription and extending process outgrowth in glia.

Keywords: FGF21, HDAC inhibitors, valproic acid, glial cells, cell processes

Introduction

Fibroblast growth factor 21 (FGF21) is a recently discovered metabolic regulator for glucose and lipids (Canto and Auwerx, 2012; Zhao et al., 2012; Li and Tang, 2015). Systemic injection of FGF21 into diabetic or overweight rodents was found to both improve insulin sensitivity and reduce weight via an interaction between FGF21 receptors and coreceptor β-Klotho (Ogawa et al., 2007; Ding

Received: December 7, 2015; **Revised:** April 6, 2016; **Accepted:** April 18, 2016

et al., 2012; Yie et al., 2012; Itoh, 2014). FGF21 expression can be induced by fasting (Mai et al., 2009; Archer et al., 2012), exercise (Berglund et al., 2010), cold (Muise et al., 2008; Hondares et al., 2011; Fisher et al., 2012), activators of PPAR-α or γ (Inagaki et al., 2007; Muise et al., 2008), the antidiabetic drug metformin, or the antihigh cholesterol drug fenofibrate (Oishi et al., 2008; Nygaard et al., 2012; Ong et al., 2012). In addition, FGF21 has been shown to promote endothelial cell-mediated angiogenesis (Inagaki et al., 2007; Yaqoob et al., 2013, 2014; Cao, 2014) and extend life span in mice (Zhang et al., 2012b). Recent studies also found that FGF21 plays a role in the brain or between the brain and systemic organs. For instance, intracerebral ventricular injection of recombinant FGF21 in rats increases hepatic insulin sensitivity and metabolic rate in diet-induced obesity (Sarruf et al., 2010). Prolonged fasting maintains glucose homeostasis through the brain-liver axis (Liang et al., 2014), while starvation induces FGF21 to act directly on the brain to lower insulin (Bookout et al., 2013) and suppress ovulation via a liver-neuroendocrine signaling pathway (Owen et al., 2013). FGF21 also has protective effects against various insults, including diabetes-induced cardiac cell death (Zhang et al., 2012a), glutamate-induced death of rat primary brain neurons (Leng et al., 2015), cardiac hypertrophy in mice (Planavila et al., 2013), sepsis toxicity in leptin-deficient ob/ob mice (Feingold et al., 2012), d-galactose-induced aging in mouse brain (Yu et al., 2015), and high glucose-induced damage and dysfunction in endothelial cells (Wang et al., 2014).

The pan-inhibitor valproic acid (VPA), which inhibits class I and IIa histone deacetylases (HDACs) (for review, see Chuang et al., 2009), is a first-line treatment drug for epilepsy (for review, see Chiu et al., 2013) and bipolar disorder (Cipriani et al., 2013). By re-modeling chromatin structure, VPA increases chaperone proteins such as heat-shock protein-70 (Ren et al., 2004; Marinova et al., 2009, 2011), glial cell line-derived neurotrophic factor (Wu et al., 2008), α-synuclein (Leng and Chuang, 2006; Monti et al., 2007), brain-derived neurotrophic factor (Yasuda et al., 2009), and vascular endothelial growth factor (Wang et al., 2012). VPA treatment also leads to functional improvement in acute and chronic neurological disease models, such as stroke (Wang et al., 2011a, 2011b), Parkinson's disease (Chen et al., 2007; Carriere et al., 2014), amyotrophic lateral sclerosis (Rouaux et al., 2007; Boll et al., 2014), Alzheimer's disease (Xuan et al., 2015), spinal cord injury (Lee et al., 2012; Lv et al., 2012; Su et al., 2014), and Huntington's disease (Zadori et al., 2009; Chiu et al., 2011). Other HDAC inhibitors that are structurally similar to VPA, including sodium butyrate (SB) and phenylbutyrate (PB), are also shown to have neuroprotective properties in primary brain neurons (Leng et al., 2008), to mitigate ischemia-induced brain damage by inducing neurogenesis and oligodendrogenesis (Kim et al., 2009; Kim and Chuang, 2014), to improve learning and memory via brain-derived neurotrophic factor-dependent mechanisms (Intlekofer et al., 2013), and to upregulate DJ-1 protein, thereby protecting neurons in animal models of Parkinson's disease (Zhou et al., 2011). Vorinostat (SAHA) and trichostatin A (TSA), which are also pan-HDAC inhibitors though structurally dissimilar to VPA, exhibit similar benefits in spinal muscular atrophy disease (Hauke et al., 2009) and improve learning and memory in mice (Sharma et al., 2015) via hyper-acetylation of histone protein to remodel chromatin.

Our laboratory recently reported that cotreatment of primary brain neurons with the mood stabilizers VPA and lithium synergistically upregulates FGF21 expression; this induction is mediated by the inhibition of HDACs and glycogen synthase kinase-3 for VPA and lithium, respectively (Leng et al., 2015). We also demonstrated that activation of the cell survival factor Akt-1 occurs upstream and downstream of FGF-21 and that both protein molecules are involved in the synergistic neuroprotective effects of VPA/lithium cotreatment in aging primary neurons (Leng et al., 2015). Interestingly, treatment of primary neurons with lithium produces small but significant effects on FGF21 expression, while VPA and other related HDAC inhibitors alone are ineffective in inducing FGF21. Despite these findings, the mechanism underlying regulation of FGF21 expression and function in brain glial cells remains unknown.

In the central nervous system (CNS), glial cells (also known as glia or neuroglia) are classified as microglia and macroglia; the latter include astrocytes, oligodendrocytes, and ependymal cells (Dong and Benveniste, 2001; Newman, 2003a). Glia are critically involved in a wide variety of neurophysiological processes. For example, astrocytes participate in repairing brain traumatic injuries (Newman, 2003b; Abbott et al., 2006; Burda et al., 2015), maintaining cellular ion balance (Obara et al., 2008), delivering nutrition to other cells (Harder et al., 2002), preserving the integrity of the blood-brain barrier (Gabryel et al., 2015), mediating neural circuitry (Khakh and Sofroniew, 2015), and protecting against CNS neuroinflammation (Sofroniew, 2015). Dysfunctional astrocytes are believed to be involved in the pathophysiology of bipolar disorder (Hercher et al., 2014), major depression (Altshuler et al., 2010; Nagy et al., 2015), autism spectrum disorder (Aida et al., 2015), and schizophrenia (Williams et al., 2013).

C6 glioma cells (C6 cells), a line originated from glial tumor in rat brain (Benda et al., 1968), exhibit astrocyte-like properties (Parker et al., 1980; Takanaga et al., 2004; Quincozes-Santos et al., 2013) and are widely used as an astrocytic cell line to study the function and regulation of brain astrocytes. This study used C6 cells and primary astrocyte-enriched glial cultures to investigate the effects of VPA and other HDAC inhibitors on FGF21 expression and to identify the HDAC isoform(s) involved in these effects. We also investigated morphological changes in glial cells associated with FGF21 overexpression.

Methods

C6 Glioma Cell Cultures

C6 cells (American Type Culture Collection, Manassas, VA), with a passage number of 45, were cultured in Dulbecco's Modified Eagle's Medium supplemented with 10% fetal bovine serum and incubated at 37°C in a humidified atmosphere containing 5% CO_2 and 95% air. Cells grown in 60-mm plates to 60% to 70% confluence were treated with mood stabilizers VPA, lithium, lamotrigine, carbamazepine, and HDAC inhibitors SB, PB, MC1568 (MC), SAHA, TSA, entinostat (MS275), apicidin, mocetinostat (Moce), or romidepsin (FK228) for 24 hours and then harvested for FGF21 mRNA analysis (VPA, lithium, lamotrigine, carbamazepine, SB, PB, SAHA, and TSA obtained from Sigma-Aldrich; MS275, apicidin, Moce, and FK228 obtained from Selleckchem). Cells grown on 25-mm circular glass cover slips were treated with the above drugs for 24 hours and stained with 0.5 μM calcein AM (Thermo Fisher Scientific), which emits a green color for live cell staining, and 5 μg/ml Hoechst 33258 (Sigma-Aldrich), which yields a blue color for cell nuclear staining (Zhu et al., 2002).

Primary Cortical Glial Cultures

All animal research was conducted according to the National Institutes of Health (NIH) Guidelines for the Care and Use of Laboratory Animals and according to procedures approved by

the NIH Animal Care and Use Committee. Cerebral cortices were dissected from 18-day-old Sprague Dawley rat embryos as previously described (Marinova et al., 2011; Leng et al., 2015). Briefly, cortices were mechanically dissociated and seeded in neurobasal growth medium (Thermo Fisher Scientific) supplemented with 15% fetal bovine serum on poly-D-lysine precoated 100-mm culture dishes or 25-mm circular glass cover slips. After 10 days in vitro, the culture consisted of a nearly neuron-free glial population, as verified by NeuN and MAP-2 antibody staining for neurons (data not shown). At approximately 60% to 70% confluence, cells were treated with VPA or other HDAC inhibitors for different experimental purposes.

Measurement and Analysis of Cell Process Length

C6 cells cultured on 25-mm cover slips were treated with the indicated drugs and then stained with the fluorescent dyes calcein AM and Hoechst 33258 to assess the length of cell processes as previously described (Howard et al., 2013). After photography with a 20× objective on a Zeiss LSM780 confocal microscope, the length of the processes was measured using ImageJ Software. Ten images of the processes in each condition were analyzed to obtain the total average length.

Total RNA Extraction and Real-Time Quantitative Polymerase Chain Reaction (qPCR)

Total RNA from cells was collected using the RNeasy Mini kit (QIAGEN). Each purified RNA sample (2 μg) was reverse-transcribed into cDNA following the instructions provided by a High Capacity cDNA Archive kit (Thermo Fisher Scientific). The reaction proceeded for 10 minutes at 25°C, 120 minutes at 37°C, and 5 minutes at 85°C. qPCR was performed using Fast Start Universal Probe master mix (Roche Applied Science) and FGF21, HDAC1, HDAC2, and HDAC3 gene expression assays (Integrated DNA Technologies). Negative controls without reverse transcriptase were included in each assay. qPCR reactions were run for 2 minutes at 50°C, 10 minutes at 95°C, 40 cycles of 15 seconds at 95°C, and 1 minute at 60°C. The $2^{-\Delta\Delta Ct}$ method was used to calculate mRNA expression levels, where C_t = cycle threshold number, ΔC_t = β-actin C_t – target gene C_t, $\Delta\Delta C_t = \Delta C_t$ control – ΔC_t treated cells, and the mRNA level of each sample was quantified relative to matched vehicle-treated controls with β-actin as the internal reference.

Western Blotting

C6 cells or cortical glial cultures grown on 60- or 100-mm dishes were detached by scraping in protein lysis buffer and then sonicated for 30 seconds (Leng et al., 2008). Protein concentration was determined with a BCA protein assay kit (Thermo Fisher Scientific). Aliquots containing equal amounts of protein (20 μg) from each sample were mixed with NuPAGE LDS sample buffer (Thermo Fisher Scientific), loaded into a 4% to 12% NuPAG Bis-Tris gel, and then subjected to electrophoresis. After separation, proteins were transferred to a nitrocellulose membrane, which was then incubated overnight at 4°C with a primary antibody against acetylated histone-H3 (AC-H3) Lys 9 and 14 (1:2000, Millipore), β-actin, acetylated tubulin (Ac-Tubulin), and total tubulin (1:10 000; Sigma-Aldrich), as well as FGF21 (1:1000, Aviscera Bioscience) in 0.1% Tween-20/phosphate-buffered saline (PBS), and then with an IRDye secondary antibody (1:10 000; LI-COR Biosciences). Reactive bands were scanned and analyzed by the Odyssey Infrared Imaging System (LI-COR Biosciences).

Specific mRNA Knockdown by Small Hairpin RNA (shRNA) and Selection of Consistent Transduced Cell Lines

C6 cells were transduced with lentivirus-mediated particles of pLKO.1-puro shRNA-control (sh-cont), shRNA-HDAC1 (sh-HDAC1), shRNA-HDAC2 (sh-HDAC2), shRNA-HDAC3 (sh-HDAC3), or shRNA-FGF21 (sh-FGF21) according to the manufacturer's protocol (Sigma-Aldrich). After 2 days, puromycin was added (6 μg/mL) to select virally transduced cells, and 7 days later cells were subcultured for different experimental purposes. The shRNA sequences for each of the targeted genes are shown in supplementary Table 1.

Lentivirus-Mediated FGF21 Overexpression

C6 cells were transduced with scramble control (Scramble) or lentivirus-mediated overexpressed FGF21 (FGF21 Overexpression) particle into which mCherry was inserted into the vector (GeneCopoeia) to yield a red color. Two days later, puromycin (1 μg/mL) was added to select transduced cells. After growing to 80% to 90% confluence, selected C6 cells were further subcultured on 60-mm dishes for western blotting to confirm protein levels of overexpressed FGF21 or onto 25-mm circular glass cover slips for studying cell process length.

Immunofluorescence Staining

Astrocyte-enriched primary cortical glia cultured on cover slips were washed with 1× PBS, then fixed with 4% paraformaldehyde (FD Neurotechnologies) for 20 minutes at room temperature, blocked with 5% goat serum for 60 minutes, and then incubated overnight at 4°C with anti-glial fibrillary acidic protein (GFAP) polyclonal antibody (1:5000, abcam) (Leng et al., 2015). After further washing with PBS, cells were incubated for 2 hours with Alexa Fluor 594-conjugated secondary antibody (1:200; Thermo Fisher Scientific), then washed with PBS and incubated in Vectashield mounting medium with 4′,6-diamidino-2-phenylindole (DAPI) (Vector Laboratories) to yield respective red and blue fluorescent images that were examined with a Zeiss LSM780 confocal microscope.

Statistical Analyses

All analyses were performed using GraphPad Prism (GraphPad). Data are expressed as means ± SEM from at least 3 independent experiments unless otherwise specified. Statistical significance was analyzed by 2-tailed unpaired *t* tests as well as 1-way ANOVA and Bonferroni's posthoc tests. $P < .05$ was considered significant.

Results

VPA Treatment Robustly Increased Levels of FGF21 mRNA and Promoted Elongation of Cell Processes in C6 Glioma Cells

C6 cells in cultures were treated with 0, 1, 2, 3, or 5 mM of VPA for 1, 2, 3, or 5 days and then harvested for qPCR assay to detect FGF21 mRNA levels. After 1 day (24 hours) treatment with VPA, FGF21 mRNA levels were increased by approximately 4-fold at 1 mM, 8-fold at 3 mM, and 16-fold at 5 mM. After 5 days of treatment, 1 mM VPA induced a near 20-fold increase of FGF21 mRNA and reached a 35-fold increase at 5 mM (Figure 1A). The effects of other mood stabilizers, namely, lithium, lamotrigine,

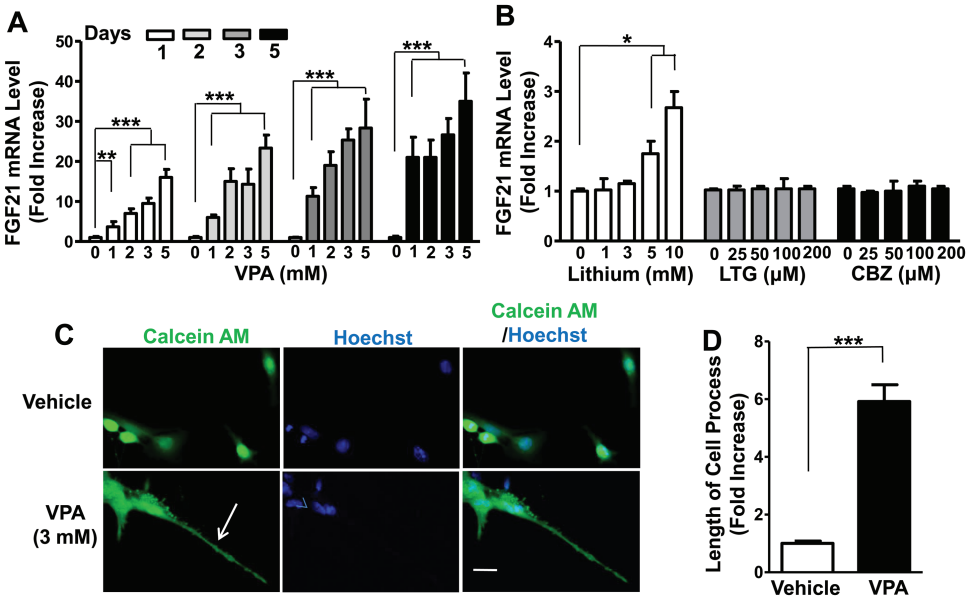

Figure 1. Treatment with valproic acid (VPA) sharply increased fibroblast growth factor 21 (FGF21) mRNA levels in a time- and concentration-dependent manner and markedly elongated process length in C6 glioma cells (C6 cells). (A) C6 cells were treated with 0, 1, 2, 3, or 5 mM VPA for the indicated number of days and harvested for FGF21 mRNA assay. (B) C6 cells were treated with indicated concentrations of lithium, lamotrigine, or carbamazepine for 24 hours and then harvested for FGF21 mRNA assay. (C) C6 cells were treated with vehicle or 3 mM VPA for 24 hours, then calcein AM (green staining) and Hoechst 33258 (blue staining) were added to live cells for 30 minutes. Bar, 50 μm. (D) Quantified results of (C) from 10 random views of each condition. Arrow, elongated cell process. Data are means ± SEM, n = 3. *P < .05, **P < .01, ***P < .001 compared with vehicle-treated control.

and carbamazepine, on FGF21 expression in C6 cells were also assessed. Lithium induced a weak (<2- to 3-fold) increase in FGF21 mRNA levels at relatively high concentrations (5 and 10 mM) after 24 hours incubation, while treatment with lamotrigine or carbamazepine in the range of 25 to 200 uM was ineffective (Figure 1B).

We also examined the effects of VPA on C6 cell morphology. VPA at different concentrations was added to C6 cells, and after 24 hours the length of cell processes was evaluated (supplementary Figure 1). Treatment with 3 mM VPA for 24 hours increased FGF21 mRNA level by approximately 9-fold (supplementary Figure 1A). At this VPA concentration, the cell process length was maximally increased by 6-fold. A higher fold of FGF21 mRNA upregulation induced by 5 or 7 mM VPA did not further increase the cell process length (supplementary Figure 1A-C), perhaps due to an "elongation saturation effect." Therefore, C6 cells were treated with 3 mM of VPA for 1 day and then exposed to calcein AM and Hoechst 33258 dyes for live cell morphological studies. The average length of cell processes measured with ImageJ Software was increased by about 6-fold after VPA treatment compared with vehicle-treated control (Figure 1C-D).

Butyrate Derivatives Also Increased FGF21 mRNA Level in C6 Cells and Promoted Elongation of Cell Processes

SB and PB are pan-HDAC inhibitors structurally and biologically similar to VPA. We found that 24-hour treatment of C6 cells with SB dose-dependently upregulated FGF21 mRNA levels by approximately 5-fold at 1 mM and 15-fold at 5 mM. FGF21 mRNA upregulation reached approximately 12- and 30-fold after 3 days of treatment with 1 and 5 mM of SB, respectively (Figure 2A). A longer duration of 5-day treatment produced even higher FGF21 mRNA increase. Treatment with PB for 1, 2, 3, or 5 days also had similar patterns on FGF21 mRNA increase compared with SB treatment (Figure 2A). We have also tested effects of MC, a purported HDAC class IIA inhibitor (Nebbioso et al., 2009; Lenoir et al., 2011). One-day treatment with MC dose-dependently increased FGF21 mRNA level, and the effect was saturated at 10 to 20 μM (Figure 2B). C6 cells were then treated with 3 mM SB, 3 mM PB, or 10 μM MC for 1 day and subsequently exposed to calcein AM and Hoechst 33258. Cell processes were markedly elongated by approximately 6-fold after these treatments compared with vehicle-treated control (Figure 2C-F).

Effects of Pan- and Class I-Specific HDAC Inhibitors on FGF21 mRNA Expression and Process Elongation in C6 Cells

SAHA and TSA inhibit HDAC class I and II and are structurally dissimilar to VPA (Chuang et al., 2009). Treatment of cells with SAHA (0.5–5 μM) for 24 hours dose-dependently elevated FGF21 mRNA levels by 20-fold at 5 μM; treatment of cells with TSA (25–200 nM) for 24 hours dose-dependently elevated FGF21 mRNA levels about 40-fold at 200 nM (Figure 3A). Parallel with these increases in FGF21 mRNA levels, the length of C6 processes was increased 6- to 7-fold by treatment with SAHA or TSA (Figure 3B-C). Other HDAC inhibitors that preferentially inhibit the activity of HDAC1, 2, or 3 isoforms (e.g., MS275, apicidin, FK228, and Moce) (Chuang et al., 2009; Nural-Guvener et al., 2015) were also tested. After 24 hours of treatment at concentrations of 0.5 μM, all these inhibitors significantly increased FGF21 mRNA levels; at 5 μM the increases were about 30-, 120-, 250-, and 190-fold for MS275, apicidin, FK228, and Moce, respectively (Figure 3D). Process lengths were also markedly increased by these 4 inhibitors (Figure 3E-F).

Effects of Pan- and Class I-Specific HDAC Inhibitors on Acetylation of Histone H3 and Tubulin

To assess the biological effects of pan-HDAC inhibitors (VPA, SB, SAHA, and TSA) and class I-specific HDAC inhibitors

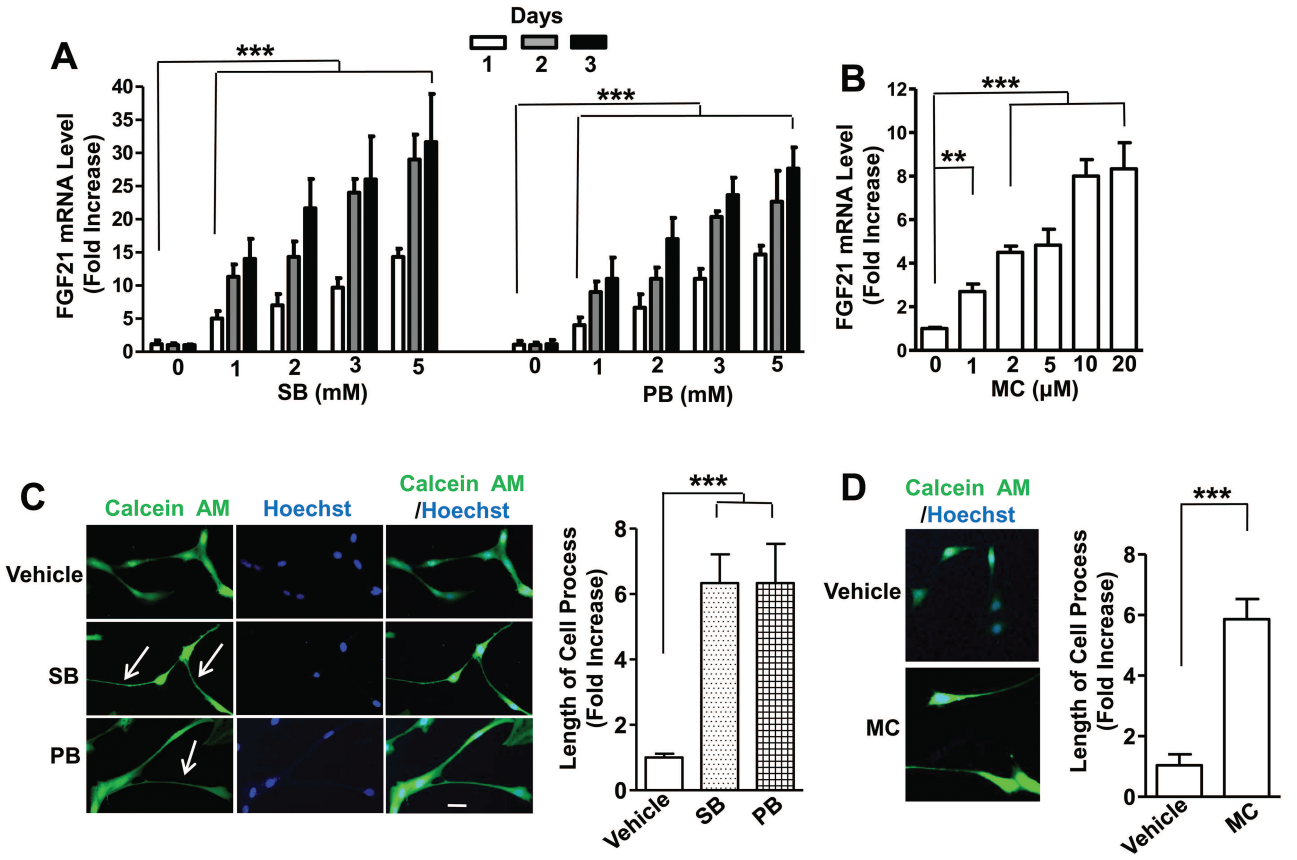

Figure 2. Treatment with sodium butyrate (SB), phenylbutyrate (PB), or MC1568 (MC) upregulated fibroblast growth factor 21 (FGF21) mRNA levels in C6 cells and significantly increased cell process length. (A) C6 cells were treated with 0, 1, 2, 3, or 5 mM SB or PB for the indicated number of days and harvested for FGF21 mRNA assay. (B) C6 cells were treated with indicated concentrations of MC for 24 hours and harvested for FGF21 mRNA assay. C6 cells were treated with vehicle, 3 mM SB, or 3 mM PB in (C), or 10 μM MC in (E). After 24 hours, calcein AM and Hoechst 33258 were added to live cells for imaging studies. Bar, 50 μm. (D) and (F) are quantified results of the length of cell processes from 10 random views of each respective treatment condition. Arrows, elongated cell processes. Data are means ± SEM, n = 3. $^{**}P < .01$, $^{***}P < .001$ compared with vehicle-treated control.

(MS275, apicidin, FK228, and Moce) on HDAC activity, C6 cells were treated with various doses of these drugs for 24 hours, then harvested for western blotting of Ac-H3 and Ac-tubulin, a target of HDAC6. VPA, SB, SAHA, and TSA treatment all robustly increased Ac-H3 levels. Ac-tubulin levels were only increased by treatment with SAHA and TSA but were unaffected by VPA and SB (Figure 4A-F). These results are consistent with the notion that SAHA and TSA inhibit class I and class II HDACs, while VPA and butyrates inhibit class I and class IIa HDACs but do not affect class IIb HDACs (e.g., HDAC6 and 10) (reviewed in Chuang et al., 2009). Treatment of C6 cells with the class I-specific HDAC inhibitors MS275, apicidin, FK228, and Moce all markedly elevated Ac-H3 levels without affecting Ac-tubulin levels in the concentration range tested (0.5–5 μM) (Figure 4G-L).

We also examined the effects of treatment with mood stabilizers on histone H3 and tubulin acetylation. Lithium (1–10 mM) did not significantly affect acetylation levels of these 2 proteins after 1 day of treatment (supplementary Figure 2A). Carbamazepine (25–200 μM) treatment modestly increased Ac-H3 levels in a dose-dependent manner, with no effects on Ac-tubulin (supplementary Figure 2B). Lamotrigine significantly increased Ac-H3 levels at 50, 100, and 200 μM (supplementary Figure 2C-D) with no significant effect at 25 μM, consistent with our previous report that this mood stabilizer is a weak and indirect HDAC inhibitor (Leng et al., 2013)

Knockdown of HDAC2 and 3, but not HDAC1, Significantly Increased FGF21 mRNA Levels and Promoted Elongation of Processes

Because the class I-specific HDAC inhibitors used in our study preferentially affect HDAC1, 2, and 3 isoforms, we used the lentivirus-mediated knockdown (gene silencing) method to identify HDAC isoform(s) involved in regulating FGF21 expression. C6 cells were transduced with lentivirus-mediated particles of sh-cont or various clones for sh-HDAC1, sh-HDAC2, or sh-HDAC3 to determine which clone had the best knockdown efficiency (supplementary Figure 3). At 48 hours, puromycin was added to select virus-transduced cells. Among various clones examined, sh-HDAC1 #439, sh-HDAC2 #397, and sh-HDAC3 #389 were found to be most effective in knocking down HDAC1, HDAC2, and HDAC3 mRNA expression, respectively, compared with other clones tested (supplementary Figure 3). Moreover, the protein levels of these HDAC isoforms were knocked down by 65%, 85%, and 70% with sh-HDAC1 #439, sh-HDAC2 #397, and sh-HDAC3 #389, respectively (supplementary Figure S4A-C). Therefore, these 3 clones were chosen for subsequent studies.

Cells transduced with HDAC2 #397 or HDAC3 #389 showed no effect on HDAC1 mRNA expression levels, in contrast to a robust knockdown with sh-HDAC1 #439 (Figure 5A). Cells transduced with sh-HDAC2 #397 showed selective knockdown on HDAC2 mRNA levels, while HDAC1 #439 had no effect and HDAC3 #389

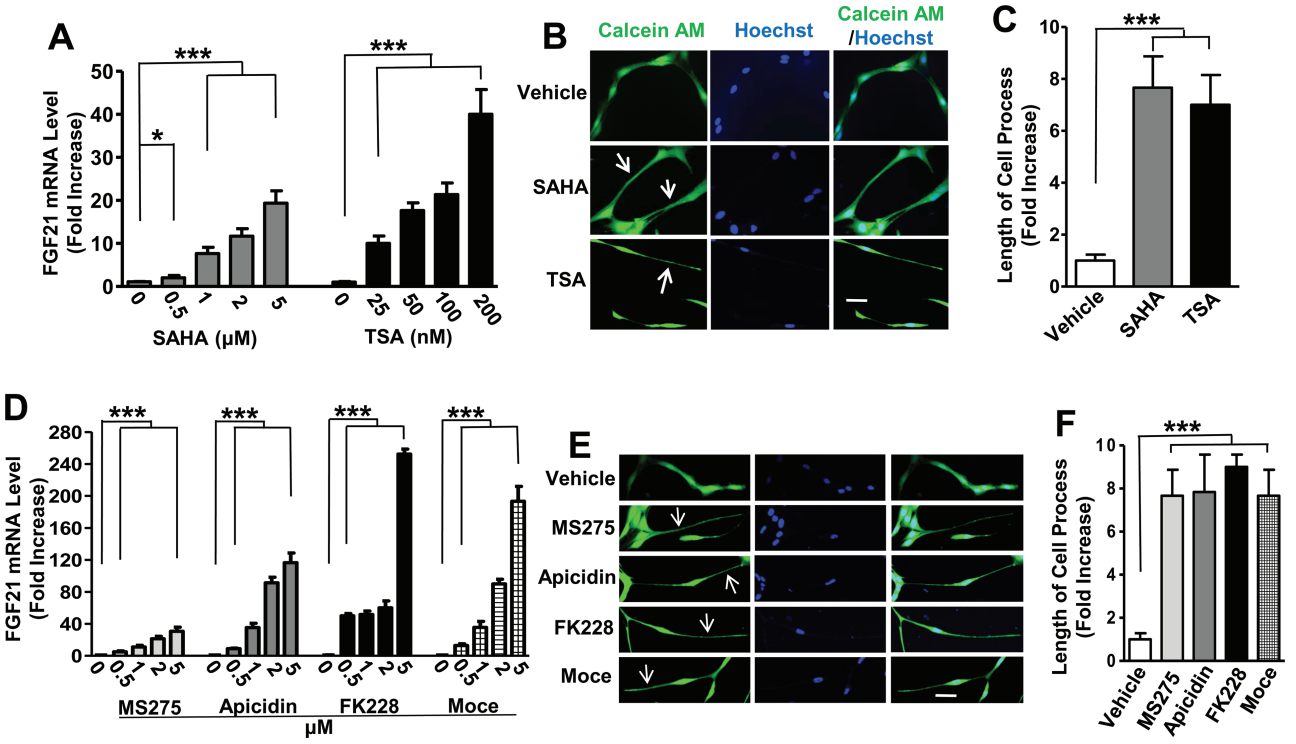

Figure 3. Treatment with vorinostat (SAHA), trichostatin A (TSA), entinostat (MS275), apicidin, romidepsin (FK228), or mocetinostat (Moce) upregulated fibroblast growth factor 21 (FGF21) mRNA levels in C6 cells and significantly increased process length. C6 cells were treated with the indicated concentrations of SAHA or TSA in (A); MS275, apicidin, MK228, or Moce in (D) for 24 hours and harvested for FGF21 mRNA assay. C6 cells were treated with 5 μM SAHA or 100 nM TSA in (B); 5 μM MS275, 1 μM apicidin, 1 μM FK228, or 1 μM Moce in (E) for 24 hours, and images were taken for calculation of process length. Bars, 50 μm. (C) and (F) are quantified results from 10 random views of each condition in B and E, respectively. Arrows, elongated cell processes. Data are means ± SEM, n = 3. *P < .05, ***P < .001 compared with vehicle-treated control.

transduction unexpectedly increased HDAC2 mRNA levels 2-fold (Figure 5B). Cells transduced with HDAC1 #439 or HDAC2 #397 had no effect on the HDAC3 mRNA expression levels as opposed to marked downregulation with sh-HDAC3 #389 (Figure 5C). Knockdown of HDAC1 had no effect on FGF21 mRNA levels, while knockdown of HDAC2 or 3 produced a nearly 8-fold and 3-fold increase, respectively (Figure 5D). Transduced C6 cells with sh-cont, sh-HDAC1, 2, and 3 were harvested for western blotting to detect Ac-H3 protein levels. Knockdown of each of these 3 isoforms significantly increased Ac-H3 levels (Figure 5E-F). Notably, knockdown of HDAC2 or 3 significantly increased the length of processes, and this was not observed with HDAC1 knockdown (Figure 5G-H). Of interest, double knockdown of HDAC2 and 3 produced additive effects on both FGF21 mRNA and C6 cell process levels (supplementary Figure 5A-C). In addition, VPA had a synergistic effect on FGF21 mRNA upregulation when used in conjunction with HDAC2 or HDAC3 knockdown (supplementary Figure 5A).

Knockdown of FGF21 Significantly Decreased the Elongated Length of Processes

C6 cells were transduced with sh-cont or sh-FGF21 #373 particle for 2 days (Leng et al., 2015). Puromycin was then added to select lentivirus-transduced cells, which were then plated for treatment with or without VPA for 24 hours. Compared to sh-cont, sh-FGF21 knocked down FGF21 mRNA levels by approximately 80% (Figure 6A). The presence of 1 or 5 mM VPA did not increase FGF21 mRNA in these knockdown conditions. Importantly, FGF21 knockdown significantly reduced VPA-induced elongation of C6 cell processes (Figure 6B-C), indicating that FGF21 is a critical mediator.

Next, we performed studies of FGF21 overexpression in C6 glioma cells. Lentivirus-mediated scramble control or FGF21 overexpression particle with mCherry inserted into the plasmid was transduced into C6 cells; 2 days later puromycin was added to kill nontransduced cells. After subculturing, cells were harvested for western blotting to confirm that FGF21 was overexpressed in C6 cells (Figure 6D). FGF21 overexpression showed an approximately 2.5-fold increase in process length in these cells (Figure 6E-F).

HDAC Inhibitors Upregulated FGF21 mRNA Levels and Promoted Elongation of Processes in Rat Primary Glial Cultures

Because C6 cells are generally considered to be an astrocytic cell line, we next studied the effects of HDAC inhibitors in astrocyte-enriched primary cortical glial cultures. Rat primary cortical glia were cultured to 50% confluency and then stained for anti-GFAP antibody to detect the percentage of astrocytes in the glia. Approximately 60% to 70% of the total glial cells were shown to be GFAP-positive astrocytes (Figure 7A). Rat primary glial cultures were treated with various concentrations of VPA for 24 hours and then harvested to assess FGF21 mRNA levels. Similar to the effects in C6 cells, VPA dose-dependently increased FGF21 mRNA levels with a significant effect at 1mM and a 7-fold elevation at 5 mM in primary glia (Figure 7B). VPA treatment did not alter FGF21 mRNA levels in rat primary cerebellar granule cells nor in cortical neurons (supplementary Figure 6). Treatment with SB (5 mM), SAHA (5 μM), or TSA (100 nM) induced a respective 3-, 7-, or 10-fold increase in FGF21 mRNA levels (Figure 7C). Western blotting revealed that protein levels of FGF21 and

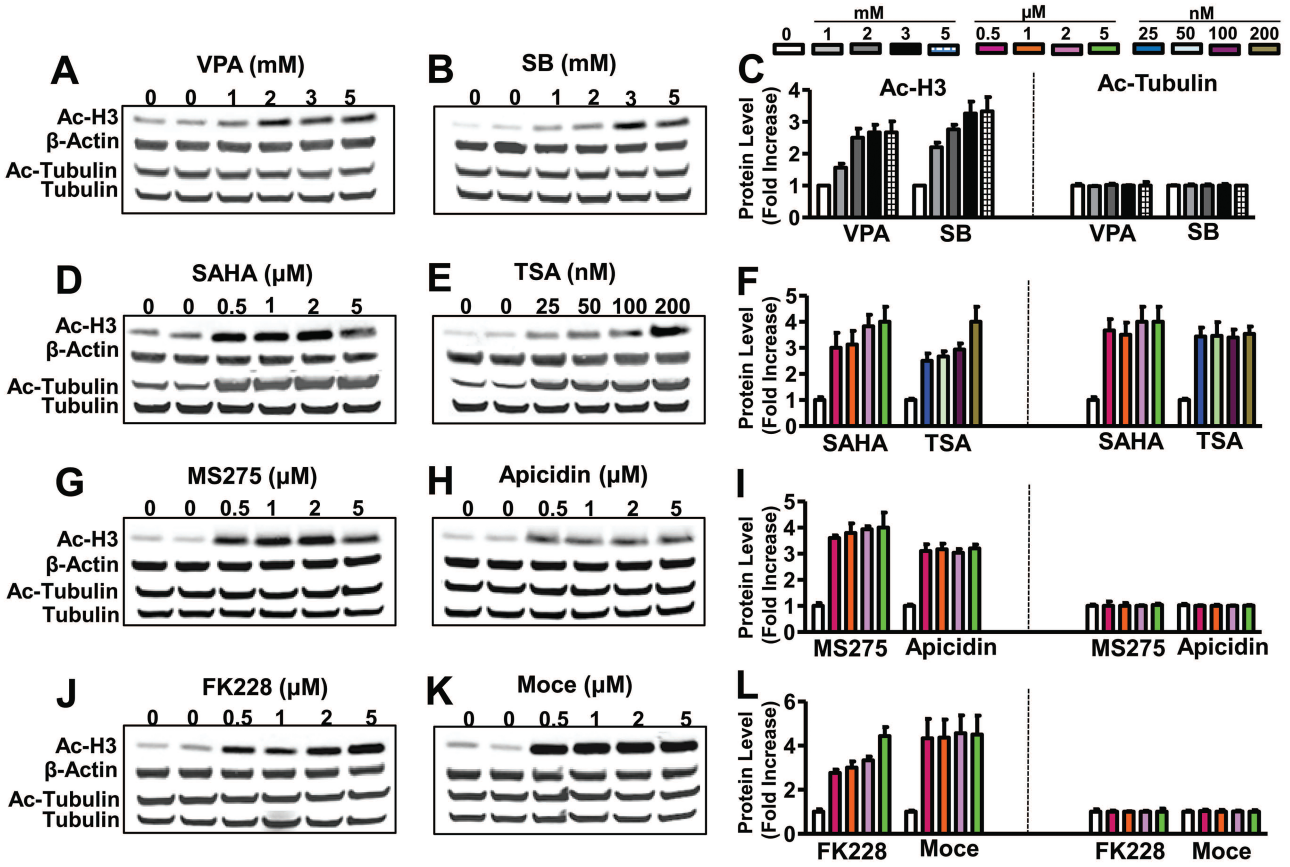

Figure 4. Treatment with valproic acid (VPA), sodium butyrate (SB), MS275, apicidin, FK228, or mocetinostat (Moce) increased acetylated histone-H3 (Ac-H3), but not acetylated tubulin (Ac-tubulin) protein levels, while treatment with vorinostat (SAHA) or trichostatin A (TSA) increased both Ac-H3 and Ac-tubulin protein levels. C6 cells were treated with indicated concentrations of VPA (A), SB (B), SAHA (D), TSA (E), MS275 (G), apicidin (H), FK228 (J), or Moce (K) for 24 hours. Cells were then lysed and processed for detection of Ac-H3, β-actin, Ac-tubulin, and total tubulin protein levels. Respective quantified data of Ac-H3 and Ac-Tubulin in each treatment condition are shown in (C), (F), (I), and (L). Quantified data are means ± SEM, n = 3.

Ac-H3 were elevated by treatment with VPA, SB, SAHA, or TSA for 48 hours, while Ac-tubulin levels were increased only by SAHA and TSA (Figure 7D). Staining of primary cortical glial cultures with anti-GFAP showed that the astrocytic processes were markedly elongated after treatment with VPA or SAHA (Figure 8A-B).

Discussion

This study is the first to demonstrate that mRNA levels of the novel metabolic regulator FGF21 can be robustly increased in C6 glioma cells and astrocyte-enriched primary cortical glial cells by treatment with VPA, a well-known mood stabilizer and anticonvulsant that is also a pan-HDAC inhibitor affecting class I (HDAC1, 2, 3, 8) and class IIa (HDAC4, 5, 7, 9) (Figure 1). Comparable FGF21 mRNA upregulation was observed by treating these cells with the structurally similar pan-HDAC inhibitors SB and PB, or with the structurally dissimilar pan-HDAC inhibitors SAHA and TSA (Figures 2 and 3). FGF21 mRNA upregulation was associated with a marked increase in the length of neurite-like processes. Lentivirus-mediated shRNA knockdown of FGF21 largely reduced VPA-induced process elongation, while FGF21 overexpression increased process length (Figure 6). These results suggest that FGF21 is a critical molecule mediating VPA-induced elongation of astrocytic processes. Our study provides additional evidence that FGF21 is not merely a factor affecting glucose and lipid metabolism in the peripheral systems; rather, its expression can be induced in brain cells including both neurons and glia with important neurobiological consequences. The robust increase in FGF21 mRNA levels in glia observed here is most likely due to hyper-acetylation of histone at the FGF21 promoter following treatment with VPA or other HDAC inhibitors. Notably, HDAC inhibition alone did not upregulate FGF21 in primary neurons (Leng et al., 2015), suggesting that there may be fundamental differences in the epigenetic regulation of FGF21 promoter activity between neurons and glial cells.

A number of HDAC inhibitors specific for HDAC1, 2 and 3 isoforms (MS275, apicidin, FK228, and Moce) were also found to strongly affect FGF21 mRNA upregulation, process extension, and Ac-H3 increase (Figures 3 and 4). shRNA-mediated knockdown experiments identified HDAC2 as the primary isoform involved in regulation of these biological effects with a lesser role of HDAC3 and no effect of HDAC1 (Figure 5). Future experiments using ChIP assay to determine the binding of HDAC2 and 3 on the FGF21 promoter will shed light on the mechanisms underlying HDAC2 and 3-mediated inhibition of FGF21 mRNA expression. Interestingly, an HDAC class IIA inhibitor MC also upregulated FGF21 mRNA and cell process length in the micro-molar dose range (Figure 2B,F). HDAC class IIA consists of HDAC4, 5, 7, and 9. Future experiments will be necessary to determine whether these biological effects of MC are indeed mediated by inhibition of HDAC IIA and, if so, the isoform involved. It is interesting that the maximal increase in the length of cell process was about

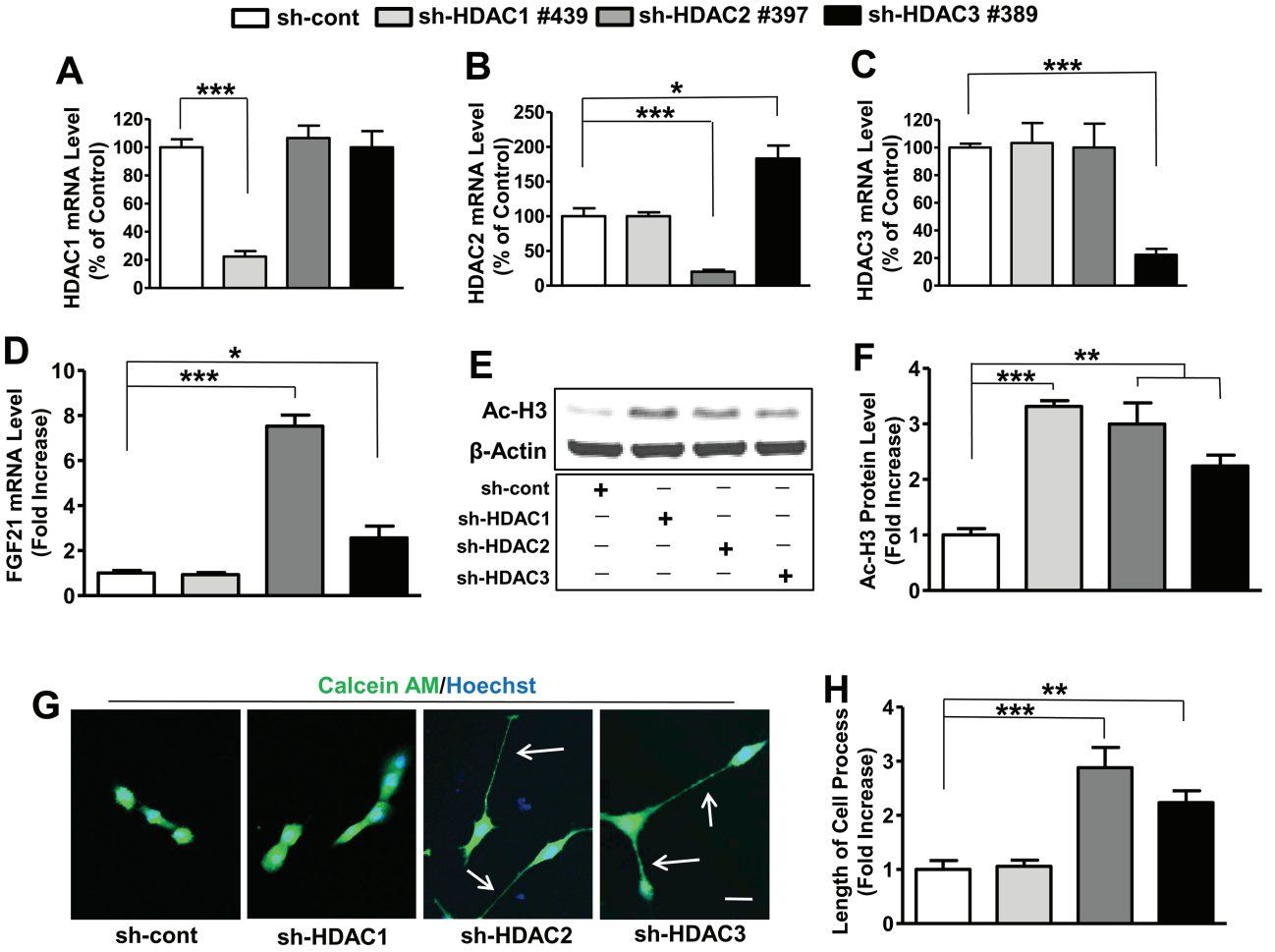

Figure 5. Knockdown of histone deacetylase 2 (HDAC2) or HDAC3, but not HDAC1, increased fibroblast growth factor 21 (FGF21) mRNA levels and promoted elongation of cell processes in C6 cells. C6 cells transduced with sh-cont, sh-HDAC1, sh-HDAC2, or sh-HDAC3 were plated on dishes, and harvested at 80% to 90% confluency for RNA or protein detection. HDAC1, 2, or 3 mRNA levels were detected as shown in (A), (B), or (C), respectively. FGF21 mRNA levels after each knockdown condition are shown in (D). Western blots of Ac-H3 and β-actin in each knockdown condition are shown in (E), and their quantified data are in (F). At 50% confluence, calcein AM and Hoechst 33258 were added to shRNA (sh)-control (sh-cont), sh-HDAC1-, sh-HDAC2-, or sh-HDAC3-transduced live C6 cells. Images were taken by confocal microscopy as shown in (G) and quantified as shown in (H). Bar, 50 μm. Arrows, elongated cell processes. Data are means ± SEM, n = 3. *P < .05, **P < .01, ***P < .001 compared with sh-cont groups.

6- to 8-fold, regardless of the diverse degree of the increase in FGF21 mRNA induced by various HDAC inhibitors including VPA, SB, PB, SAHA, TSA, MS275, apicidin, FK288, Moce, and MC. Based on the data in this report, we suggest that an elevation of FGF21 mRNA of approximately 10-fold by various inhibitors is sufficient to induce a maximal increase in the length of cell process, and an additional increase in FGF21 mRNA fails to further elongate cell processes, as the effect has been saturated.

It should be noted that the extent of FGF21 upregulation and process elongation induced by HDAC2 or HDAC3 knockdown was considerably smaller than those induced by pharmacological treatment (Figures 1–5). These observations may be attributed to incomplete knockdown of HDAC isoforms or, alternately, may suggest that concurrent inhibition of other HDAC isoforms may potentiate the biological effects resulting from HDAC2 or HDAC3 inhibition. Other studies noted that HDAC2 knockout mice showed improved memory in a mouse model of Alzheimer's disease (Guan et al., 2009). Conversely, mice overexpressing HDAC2, but not HDAC1, exhibit impaired memory in conjunction with decreased dendrite spine density and synaptic formation in the hippocampus. HDAC2 also appears to negatively regulate synaptic plasticity by binding to the promoters of a spectrum of genes involved in neuronal activity to suppress their expression (Guan et al., 2009). Selective knockout of HDAC2 in forebrain neurons was also reported to improve working memory and accelerate extinction learning (Morris et al., 2013). HDAC2 inhibition also appears to be involved in the antidepressant-like effects of SB (Han et al., 2014). Higher HDAC2-mediated histone modifications in the amygdala are thought to predispose individuals to anxiety and alcoholism (Moonat et al., 2013). In addition, HDAC2 regulates atypical antipsychotic responses via mGlu2 promoter modulation (Kurita et al., 2012), suggesting that HDAC2 is a promising new target for schizophrenia treatment.

The importance of the interactions between glia and neurons is increasingly recognized (Araque et al., 1999; Perea et al., 2009). The term tripartite synapse refers to the structure formed by pre- and postsynapses and the process branches of astrocytes. Under electron microscopy, astrocyte processes were found to wrap the spine synapses of neurons (Khakh and Sofroniew, 2015; Verkhratsky et al., 2015). The robust FGF21-dependent elongation of astrocytic processes observed in our study suggests that these may enhance interactions with neurons and promote tripartite synapse formation as well as other

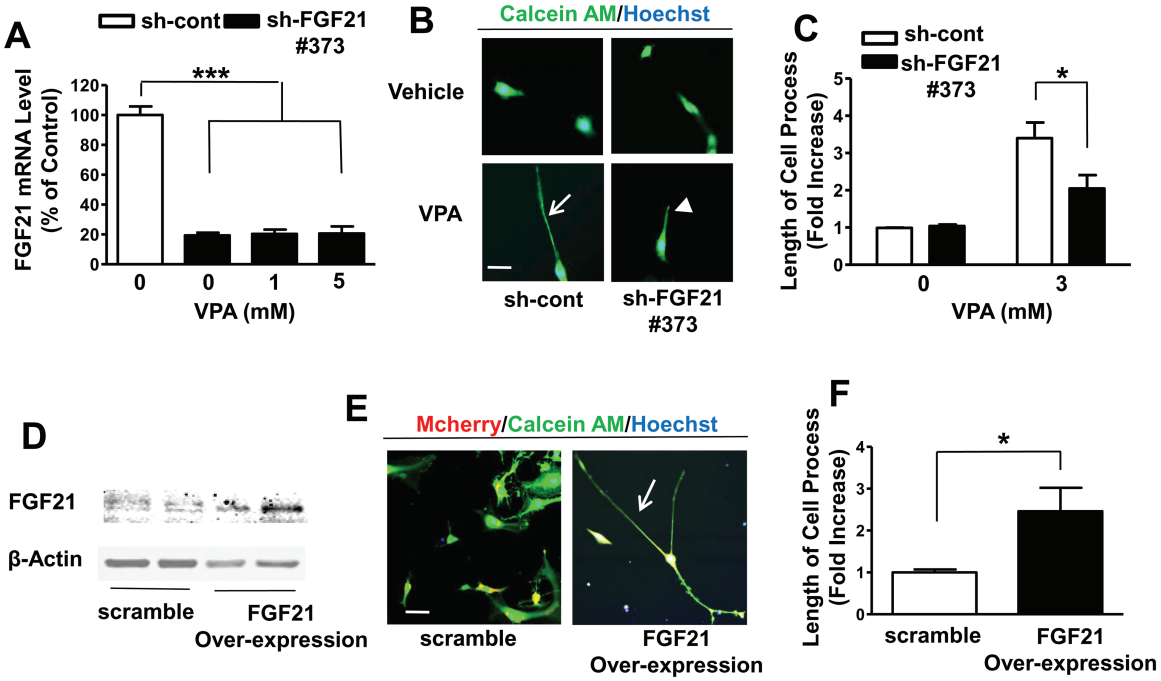

Figure 6. Valproic acid (VPA)-induced upregulation of fibroblast growth factor 21 (FGF21) mRNA levels and increased length of cell processes were significantly abolished by knock-down of FGF21, while overexpression of recombinant FGF21 boosted the length of cell processes in C6 cells. C6 cells with transduced shRNA (sh)-control (sh-cont), or sh-FGF21 #373 were treated with 1 or 5 mM VPA for 24 hours and harvested for detection of FGF21 mRNA levels as shown in (A). Transduced C6 cells were treated with 3 mM VPA for 24 hours, cell processes were imaged by adding calcein AM and Hoechst 33258 as shown in (B) and quantified as shown in (C). C6 transduced with scramble control or lentivirus-mediated overexpressed FGF21 particles were harvested for western blotting (D) or photographed by confocal microscopy (E) with quantified results as shown in (F). Bar, 50 μm. Arrows for elongated, and arrow-head for shortened cell processes. Data are means ± SEM, n = 3. $P < .05$, $^{***}P < .001$ compared with control group.

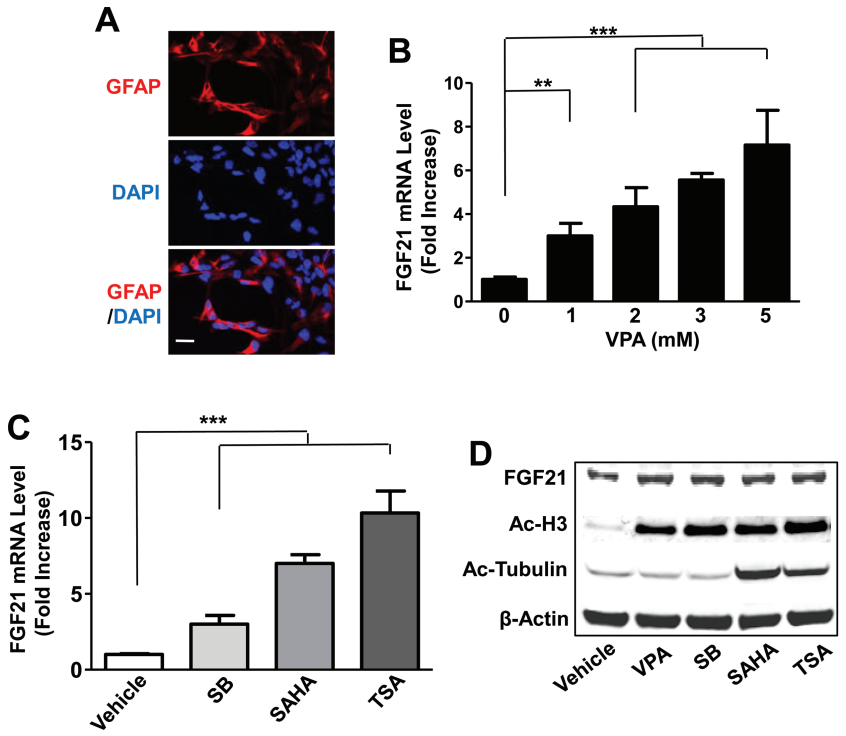

Figure 7. Fibroblast growth factor 21 (FGF21) mRNA levels were increased by valproic acid (VPA) and other histone deacetylase (HDAC) inhibitors in primary cortical glia cultures. Primary cortical glial cultures were incubated with anti-GFAP antibody and mounted with medium containing DAPI and then photographed with a confocal microscope (A). Bar, 50 μm. Cortical glial cultures were treated with indicated concentrations of VPA (B), 5 mM sodium butyrate (SB), 5 μM vorinostat (SAHA), or 100 nM trichostatin A (TSA) (C) for 24 hours and harvested for FGF21 mRNA detection. Cortical glial cultures were treated with 5 mM VPA, 5 mM SB, 5 μM SAHA, or 100 nM TSA for 48 hours and harvested for Western blotting detection (D). Data in B and C are means ± SEM, n = 3. $^{**}P < .01$, $^{***}P < .001$ compared with vehicle-treated control.

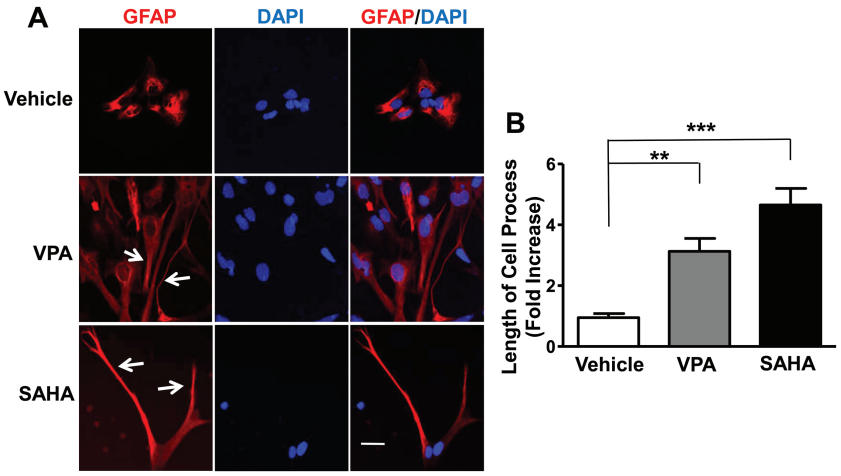

Figure 8. Valproic acid (VPA) and vorinostat (SAHA) treatment increased the length of astrocyte processes. Rat cortical glial cultures were treated with 3 mM VPA or 5 μM SAHA for 48 hours, fixed and stained for anti-GFAP antibody (which recognizes astrocytes), then mounted with medium containing DAPI for nuclei staining. The morphology of GFAP-positive cells was examined by confocal microscopy (A). Bar, 50 μm. The lengths of the processes of GFAP-positive astrocytes were determined from 6 random views of each treatment condition (B). Quantified data are means ± SEM, n = 3. **P < .01, ***P < .001 compared with vehicle-treated control.

neuronal activities in the brain. Morphological alteration of prefrontal glia has been found in bipolar disorder and schizophrenia (Hercher et al., 2014), and astrocytic abnormalities have also been reported in the brain of depression and suicide victims (Nagy et al., 2015). Given that the FGF family has been strongly implicated as a neuromodulator in affective disorders (Turner et al., 2012), it seems possibile that VPA-induced FGF21 expression and process elongation in astrocytes may contribute to the clinical efficay of this drug in treating bipolar disorder.

In addition to mood disorders, VPA also has beneficial effects in a variety of neurodegeneative, neurological, and neuropsychiatric diseases (for review, see Chiu et al., 2013). Other HDAC inhibitors used in this study have also been reported to have benefits in various preclinical models of brain disorders. For example, SB and TSA reduce brain infarction and neurological deficits in experimental stroke animals (Kim et al., 2009; Kim and Chuang, 2014), and TSA also improves symptoms in mouse models of spinal muscular atrophy (Rouaux et al., 2004; Liu et al., 2014). SAHA improves synaptic plasticity and memory formation in a mouse model of Alzheimer's disease (Guan et al., 2009). MS275 has been shown to improve cognitive performance and reduce cell death following traumatic brain injury in rats (Cao et al., 2013), to rescue brain structural and functional deficits in a mouse model of Kabuki syndrome (Bjornsson et al., 2014), and to protect against injury of ganglionic cells in mouse retina (Chindasub et al., 2013). Finally, FK228 normalizes axonal transport defects in an Alzheimer's disease model (Johnson et al., 2013). Further investigation is needed to explore whether the advantageous effects of these HDAC inhibitors involve FGF21 induction and process extension in brain astrocytes.

In conclusion, this study showed that VPA and other HDAC inhibitors robustly increase FGF21 mRNA levels and process lengths in an astrocytic cell line as well as in astrocyte-enriched cortical glial cultures. We also provided evidence that HDAC2 and HDAC3 isoforms are involved in mediating both biological effects and that FGF21 is a critical mediator for process elongation. These novel results support a previously undescribed role for FGF21 in the nervous system and suggest a potential new mechanism underlying the protective role of HDAC inhibition in CNS pathological conditions.

Acknowledgments

The authors thank Drs. Francis McMahon and Carolyn B Smith (NIMH, NIH) for their guidance and support, the members of the Molecular Neurobiology Section (NIMH, NIH) for their helpful discussions and assistance, and Ioline Henter (NIMH, NIH) for critical review and editorial assistance with this manuscript.

This study was supported by the Intramural Research Program of the National Institute of Mental Health, National Institutes of Health (1ZIAMH002468-25). This work was written as part of the authors' official duties as Government employees (affiliated with Annual Report ZIAMH002468). The views expressed in this article do not necessarily represent the views of the NIMH, NIH, HHS, or the United States Government.

Statement of Interest

None.

References

Abbott NJ, Ronnback L, Hansson E (2006) Astrocyte-endothelial interactions at the blood-brain barrier. Nat Rev Neurosci 7:41–53.

Aida T, Yoshida J, Nomura M, Tanimura A, Iino Y, Soma M, Bai N, Ito Y, Cui W, Aizawa H, Yanagisawa M, Nagai T, Takata N, Tanaka KF, Takayanagi R, Kano M, Gotz M, Hirase H, Tanaka K (2015) Astroglial glutamate transporter deficiency increases synaptic excitability and leads to pathological repetitive behaviors in mice. Neuropsychopharmacol 40:1569–1579.

Altshuler LL, Abulseoud OA, Foland-Ross L, Bartzokis G, Chang S, Mintz J, Hellemann G, Vinters HV (2010) Amygdala astrocyte reduction in subjects with major depressive disorder but not bipolar disorder. Bipolar Disord 12:541–549.

Araque A, Parpura V, Sanzgiri RP, Haydon PG (1999) Tripartite synapses: glia, the unacknowledged partner. Trends Neurosci 22:208–215.

Archer A, Venteclef N, Mode A, Pedrelli M, Gabbi C, Clement K, Parini P, Gustafsson JA, Korach-Andre M (2012) Fasting-induced FGF21 is repressed by LXR activation via recruitment of an HDAC3 corepressor complex in mice. Mol Endocrinol 26:1980–1990.

Benda P, Lightbody J, Sato G, Levine L, Sweet W (1968) Differentiated rat glial cell strain in tissue culture. Science 161:370–371.

Berglund ED, Kang L, Lee-Young RS, Hasenour CM, Lustig DG, Lynes SE, Donahue EP, Swift LL, Charron MJ, Wasserman DH (2010) Glucagon and lipid interactions in the regulation of hepatic AMPK signaling and expression of PPAR alpha and FGF21 transcripts in vivo. Am J Physiol-Endoc Metab 299:E607–E614.

Bjornsson HT, Benjamin JS, Zhang L, Weissman J, Gerber EE, Chen YC, Vaurio RG, Potter MC, Hansen KD, Dietz HC (2014) Histone deacetylase inhibition rescues structural and functional brain deficits in a mouse model of Kabuki syndrome. Sci Translat Med 6:256ra135.

Boll MC, Bayliss L, Vargas-Canas S, Burgos J, Montes S, Penaloza-Solano G, Rios C, Alcaraz-Zubeldia M (2014) Clinical and biological changes under treatment with lithium carbonate and valproic acid in sporadic amyotrophic lateral sclerosis. J Neurol Sci 340:103–108.

Bookout AL, de Groot MHM, Owen BM, Lee S, Gautron L, Lawrence HL, Ding XS, Elmquist JK, Takahashi JS, Mangelsdorf DJ, Kliewer SA (2013) FGF21 regulates metabolism and circadian behavior by acting on the nervous system. Nat Med 19:1147–1152.

Burda JE, Bernstein AM, Sofroniew MV (2015) Astrocyte roles in traumatic brain injury. Exp Neurol 275:305–315.

Canto C, Auwerx J (2012) FGF21 Takes a fat bite. Science 336:675–676.

Cao P, Liang Y, Gao X, Zhao MG, Liang GB (2013) Administration of MS-275 improves cognitive performance and reduces cell death following traumatic brain injury in rats. CNS Neurosci Ther 19:337–345.

Cao S (2014) FGF21 promotes angiogenesis through endocytosis dependent activation of FGFR1 in endothelial cells. Angiogenesis 17:300–300.

Carriere CH, Kang NH, Niles LP (2014) Neuroprotection by valproic acid in an intrastriatal rotenone model of Parkinson's disease. Neuroscience 267:114–121.

Chen PS, Wang CC, Bortner CD, Peng GS, Wu X, Pang H, Lu RB, Gean PW, Chuang DM, Hong JS (2007) Valproic acid and other histone deacetylase inhibitors induce microglial apoptosis and attenuate lipopolysaccharide-induced dopaminergic neurotoxicity. Neuroscience 149:203–212.

Chindasub P, Lindsey JD, Duong-Polk K, Leung CK, Weinreb RN (2013) Inhibition of histone deacetylases 1 and 3 protects injured retinal ganglion cells. Invest Ophthalmol Vis Sci 54:96–102.

Chiu CT, Liu GP, Leeds P, Chuang DM (2011) Combined treatment with the mood stabilizers lithium and valproate produces multiple beneficial effects in transgenic mouse models of Huntington's Disease. Neuropsychopharmacol 36:2406–2421.

Chiu CT, Wang Z, Hunsberger JG, Chuang DM (2013) Therapeutic potential of mood stabilizers lithium and valproic acid: beyond bipolar disorder. Pharmacol Rev 65:105–142.

Chuang DM, Leng Y, Marinova Z, Kim HJ, Chiu CT (2009) Multiple roles of HDAC inhibition in neurodegenerative conditions. Trends Neurosci 32:591–601.

Cipriani A, Reid K, Young AH, Macritchie K, Geddes J (2013) Valproic acid, valproate and divalproex in the maintenance treatment of bipolar disorder. Cochrane Database Syst Rev 10:CD003196.

Ding X, Boney-Montoya J, Owen BM, Bookout AL, Coate KC, Mangelsdorf DJ, Kliewer SA (2012) betaKlotho is required for fibroblast growth factor 21 effects on growth and metabolism. Cell Metab 16:387–393.

Dong Y, Benveniste EN (2001) Immune function of astrocytes. Glia 36:180–190.

Feingold KR, Grunfeld C, Heuer JG, Gupta A, Cramer M, Zhang TH, Shigenaga JK, Patzek SM, Chan ZW, Moser A, Bina H, Kharitonenkov A (2012) FGF21 is increased by inflammatory stimuli and protects leptin-deficient ob/ob mice from the toxicity of sepsis. Endocrinology 153:2689–2700.

Fisher FM, Kleiner S, Douris N, Fox EC, Mepani RJ, Verdeguer F, Wu J, Kharitonenkov A, Flier JS, Maratos-Flier E, Spiegelman BM (2012) FGF21 regulates PGC-1 alpha and browning of white adipose tissues in adaptive thermogenesis. Gene Dev 26:271–281.

Gabryel B, Kasprowska D, Kost A, Labuzek K, Urbanek T (2015) [Astrocytes in ischemic stroke - a potential target for neuroprotective strategies]. Postepy Hig Med Dosw 69:384–397.

Guan JS, Haggarty SJ, Giacometti E, Dannenberg JH, Joseph N, Gao J, Nieland TJ, Zhou Y, Wang X, Mazitschek R, Bradner JE, DePinho RA, Jaenisch R, Tsai LH (2009) HDAC2 negatively regulates memory formation and synaptic plasticity. Nature 459:55–60.

Han A, Sung YB, Chung SY, Kwon MS (2014) Possible additional antidepressant-like mechanism of sodium butyrate: targeting the hippocampus. Neuropharmacology 81:292–302.

Harder DR, Zhang C, Gebremedhin D (2002) Astrocytes function in matching blood flow to metabolic activity. News Physiol Sci 17:27–31.

Hauke J, Riessland M, Lunke S, Eyupoglu IY, Blumcke I, El-Osta A, Wirth B, Hahnen E (2009) Survival motor neuron gene 2 silencing by DNA methylation correlates with spinal muscular atrophy disease severity and can be bypassed by histone deacetylase inhibition. Hum Mol Genet 18:304–317.

Hercher C, Chopra V, Beasley CL (2014) Evidence for morphological alterations in prefrontal white matter glia in schizophrenia and bipolar disorder. J Psych Neurosci 39:376–385.

Hondares E, Iglesias R, Giralt A, Gonzalez FJ, Giralt M, Mampel T, Villarroya F (2011) Thermogenic activation induces FGF21 expression and release in brown adipose tissue. J Biol Chem 286:12983–12990.

Howard L, Wyatt S, Nagappan G, Davies AM (2013) ProNGF promotes neurite growth from a subset of NGF-dependent neurons by a p75NTR-dependent mechanism. Development 140:2108–2117.

Inagaki T, Dutchak P, Zhao G, Ding X, Gautron L, Parameswara V, Li Y, Goetz R, Mohammadi M, Esser V, Elmquist JK, Gerard RD, Burgess SC, Hammer RE, Mangelsdorf DJ, Kliewer SA (2007) Endocrine regulation of the fasting response by PPARalpha-mediated induction of fibroblast growth factor 21. Cell Metabolism 5:415–425.

Intlekofer KA, Berchtold NC, Malvaez M, Carlos AJ, McQuown SC, Cunningham MJ, Wood MA, Cotman CW (2013) Exercise and sodium butyrate transform a subthreshold learning event into long-term memory via a brain-derived neurotrophic factor-dependent mechanism. Neuropsychopharmacol 38:2027–2034.

Itoh N (2014) FGF21 as a hepatokine, adipokine, and myokine in metabolism and diseases. Front Endocrinol 5:107.

Johnson AA, Sarthi J, Pirooznia SK, Reube W, Elefant F (2013) Increasing Tip60 HAT levels rescues axonal transport defects and associated behavioral phenotypes in a Drosophila Alzheimer's disease model. J Neurosci 33:7535–7547.

Khakh BS, Sofroniew MV (2015) Diversity of astrocyte functions and phenotypes in neural circuits. Nat Neurosci 18:942–952.

Kim HJ, Chuang DM (2014) HDAC inhibitors mitigate ischemia-induced oligodendrocyte damage: potential roles of oligodendrogenesis, VEGF, and anti-inflammation. Am J Transl Res 6:206–223.

Kim HJ, Leeds P, Chuang DM (2009) The HDAC inhibitor, sodium butyrate, stimulates neurogenesis in the ischemic brain. J Neurochem 110:1226–1240.

Kurita M, Holloway T, García-Bea A, Kozlenkov A, Friedman AK, Moreno JL, Heshmati M, Golden SA, Kennedy PJ, Takahashi N, Dietz DM, Mocci G, Gabilondo AM, Hanks J, Umali A, Callado LF, Gallitano AL, Neve RL, Shen L, Buxbaum JD, Han MH, Nestler EJ, Meana JJ, Russo SJ, González-Maeso J. (2012) HDAC2 regulates atypical antipsychotic responses through the modulation of mGlu2 promoter activity. Nat Neurosci 15:1245–1254.

Lee JY, Kim HS, Choi HY, Oh TH, Ju BG, Yune TY (2012) Valproic acid attenuates blood-spinal cord barrier disruption by inhibiting matrix metalloprotease-9 activity and improves functional recovery after spinal cord injury. J Neurochem 121:818–829.

Leng Y, Chuang DM (2006) Endogenous alpha-synuclein is induced by valproic acid through histone deacetylase inhibition and participates in neuroprotection against glutamate-induced excitotoxicity. J Neurosci 26:7502–7512.

Leng Y, Fessler EB, Chuang DM (2013) Neuroprotective effects of the mood stabilizer lamotrigine against glutamate excitotoxicity: roles of chromatin remodelling and Bcl-2 induction. Int J Neuropsychopharmacol 16:607–620.

Leng Y, Liang MH, Ren M, Marinova Z, Leeds P, Chuang DM (2008) Synergistic neuroprotective effects of lithium and valproic acid or other histone deacetylase inhibitors in neurons: roles of glycogen synthase kinase-3 inhibition. J Neurosci 28:2576–2588.

Leng Y, Wang Z, Tsai LK, Leeds P, Fessler EB, Wang J, Chuang DM (2015) FGF-21, a novel metabolic regulator, has a robust neuroprotective role and is markedly elevated in neurons by mood stabilizers. Mol Psychiatr 20:215–223.

Lenoir O, Flosseau K, Ma FX, Blondeau B, Mai A, Bassel-Duby R, Ravassard P, Olson EN, Haumaitre C, Scharfmann R (2011) Specific control of pancreatic endocrine beta- and delta-cell mass by class IIa histone deacetylases HDAC4, HDAC5, and HDAC9. Diabetes 60:2861–2871.

Li LI, Tang L (2015) Multiple roles of fibroblast growth factor 21 in metabolism. Curr Pharm Des 21:3041–3050.

Liang QN, Zhong L, Zhang JL, Wang Y, Bornstein SR, Triggle CR, Ding H, Lam KSL, Xu AM (2014) FGF21 maintains glucose homeostasis by mediating the cross talk between liver and brain during prolonged fasting. Diabetes 63:4064–4075.

Liu H, Yazdani A, Murray LM, Beauvais A, Kothary R (2014) The Smn-independent beneficial effects of trichostatin A on an intermediate mouse model of spinal muscular atrophy. Plos One 9:e101225.

Lv L, Han X, Sun Y, Wang X, Dong Q (2012) Valproic acid improves locomotion in vivo after SCI and axonal growth of neurons in vitro. Exp Neurol 233:783–790.

Mai K, Andres J, Biedasek K, Weicht J, Bobbert T, Sabath M, Meinus S, Reinecke F, Mohlig M, Weickert MO, Clemenz M, Pfeiffer AF, Kintscher U, Spuler S, Spranger J (2009) Free fatty acids link metabolism and regulation of the insulin-sensitizing fibroblast growth factor-21. Diabetes 58:1532–1538.

Marinova Z, Leng Y, Leeds P, Chuang DM (2011) Histone deacetylase inhibition alters histone methylation associated with heat shock protein 70 promoter modifications in astrocytes and neurons. Neuropharmacology 60:1109–1115.

Marinova Z, Ren M, Wendland JR, Leng Y, Liang MH, Yasuda S, Leeds P, Chuang DM (2009) Valproic acid induces functional heat-shock protein 70 via class I histone deacetylase inhibition in cortical neurons: a potential role of Sp1 acetylation. J Neurochem 111:976–987.

Monti B, Polazzi E, Batti L, Crochemore C, Virgili M, Contestabile A (2007) Alpha-synuclein protects cerebellar granule neurons against 6-hydroxydopamine-induced death. J Neurochem 103:518–530.

Moonat S, Sakharkar AJ, Zhang H, Tang L, Pandey SC (2013) Aberrant histone deacetylase2-mediated histone modifications and synaptic plasticity in the amygdala predisposes to anxiety and alcoholism. Biol Psychiatry 73:763–773.

Morris MJ, Mahgoub M, Na ES, Pranav H, Monteggia LM (2013) Loss of histone deacetylase 2 improves working memory and accelerates extinction learning. J Neurosci 33:6401–6411.

Muise ES, Azzolina B, Kuo DW, El-Sherbeini M, Tan Y, Yuan X, Mu J, Thompson JR, Berger JP, Wong KK (2008) Adipose fibroblast growth factor 21 is up-regulated by peroxisome proliferator-activated receptor gamma and altered metabolic states. Mol Pharmacol 74:403–412.

Nagy C, Suderman M, Yang J, Szyf M, Mechawar N, Ernst C, Turecki G (2015) Astrocytic abnormalities and global DNA methylation patterns in depression and suicide. Mol Psychiatry 20:320–328.

Nebbioso A, Manzo F, Miceli M, Conte M, Manente L, Baldi A, De Luca A, Rotili D, Valente S, Mai A, Usiello A, Gronemeyer H, Altucci L (2009) Selective class II HDAC inhibitors impair myogenesis by modulating the stability and activity of HDAC-MEF2 complexes. Embo Rep 10:776–782.

Newman EA (2003a) Glial cell inhibition of neurons by release of ATP. J Neurosci 23:1659–1666.

Newman EA (2003b) New roles for astrocytes: regulation of synaptic transmission. Trends Neurosci 26:536–542.

Nural-Guvener H, Zakharova L, Feehery L, Sljukic S, Gaballa M (2015) Anti-fibrotic effects of class I HDAC inhibitor, mocetinostat is associated with IL-6/Stat3 signaling in ischemic heart failure. Int J Mol Sci 16:11482–11499.

Nygaard EB, Vienberg SG, Orskov C, Hansen HS, Andersen B (2012) Metformin stimulates FGF21 expression in primary hepatocytes. Exp Diabetes Res 2012:465282.

Obara M, Szeliga M, Albrecht J (2008) Regulation of pH in the mammalian central nervous system under normal and pathological conditions: facts and hypotheses. Neurochem Int 52:905–919.

Ogawa Y, Kurosu H, Yamamoto M, Nandi A, Rosenblatt KP, Goetz R, Eliseenkova AV, Mohammadi M, Kuro-o M (2007) beta Klotho is required for metabolic activity of fibroblast growth factor 21. P Natl Acad Sci USA 104:7432–7437.

Oishi K, Uchida D, Ishida N (2008) Circadian expression of FGF21 is induced by PPAR alpha activation in the mouse liver. Febs Lett 582:3639–3642.

Ong KL, Rye KA, O'Connell R, Jenkins AJ, Brown C, Xu A, Sullivan DR, Barter PJ, Keech AC, investigators Fs (2012) Long-term fenofibrate therapy increases fibroblast growth factor 21 and retinol-binding protein 4 in subjects with type 2 diabetes. J Clin Endocrinol Metab 97:4701–4708.

Owen BM, Bookout AL, Ding XS, Lin VY, Atkin SD, Gautron L, Kliewer SA, Mangelsdorf DJ (2013) FGF21 contributes to neuroendocrine control of female reproduction. Nat Med 19:1153–1156.

Parker KK, Norenberg MD, Vernadakis A (1980) "Transdifferentiation" of C6 glial cells in culture. Science 208:179–181.

Perea G, Navarrete M, Araque A (2009) Tripartite synapses: astrocytes process and control synaptic information. Trends Neurosci 32:421–431.

Planavila A, Redondo I, Hondares E, Vinciguerra M, Munts C, Iglesias R, Gabrielli LA, Sitges M, Giralt M, van Bilsen M, Villarroya F (2013) Fibroblast growth factor 21 protects against cardiac hypertrophy in mice. Nat Commun 4:2019.

Quincozes-Santos A, Bobermin LD, Latini A, Wajner M, Souza DO, Goncalves CA, Gottfried C (2013) Resveratrol protects C6 astrocyte cell line against hydrogen peroxide-induced oxidative stress through heme oxygenase 1. Plos One 8:e64372.

Ren M, Leng Y, Jeong M, Leeds PR, Chuang DM (2004) Valproic acid reduces brain damage induced by transient focal cerebral ischemia in rats: potential roles of histone deacetylase inhibition and heat shock protein induction. J Neurochem 89:1358–1367.

Rouaux C, Loeffler JP, Boutillier AL (2004) Targeting CREB-binding protein (CBP) loss of function as a therapeutic strategy in neurological disorders. Biochem Pharmacol 68:1157–1164.

Rouaux C, Panteleeva I, Rene F, Gonzalez de Aguilar JL, Echaniz-Laguna A, Dupuis L, Menger Y, Boutillier AL, Loeffler JP (2007) Sodium valproate exerts neuroprotective effects in vivo through CREB-binding protein-dependent mechanisms but does not improve survival in an amyotrophic lateral sclerosis mouse model. J Neurosci 27:5535–5545.

Sarruf DA, Thaler JP, Morton GJ, German J, Fischer JD, Ogimoto K, Schwartz MW (2010) Fibroblast growth factor 21 action in the brain increases energy expenditure and insulin sensitivity in obese rats. Diabetes 59:1817–1824.

Sharma S, Taliyan R, Ramagiri S (2015) Histone deacetylase inhibitor, trichostatin A, improves learning and memory in high-fat diet-induced cognitive deficits in mice. J Mol Neurosci 56:1–11.

Sofroniew MV (2015) Astrocyte barriers to neurotoxic inflammation. Nat Rev Neurosci 16:249–263.

Su Z, Niu W, Liu ML, Zou Y, Zhang CL (2014) In vivo conversion of astrocytes to neurons in the injured adult spinal cord. Nat Commun 5:3338.

Takanaga H, Yoshitake T, Hara S, Yamasaki C, Kunimoto M (2004) cAMP-induced astrocytic differentiation of C6 glioma cells is mediated by autocrine interleukin-6. J Biol Chem 279:15441–15447.

Turner CA, Watson SJ, Akil H (2012) The fibroblast growth factor family: neuromodulation of affective behavior. Neuron 76:160–174.

Verkhratsky A, Nedergaard M, Hertz L (2015) Why are astrocytes important? Neurochem Res 40:389–401.

Wang XM, Song SS, Xiao H, Gao P, Li XJ, Si LY (2014) Fibroblast growth factor 21 protects against high glucose induced cellular damage and dysfunction of endothelial nitric-oxide synthase in endothelial cells. Cell Physiol Biochem 34:658–671.

Wang Z, Tsai LK, Munasinghe J, Leng Y, Fessler EB, Chibane F, Leeds P, Chuang DM (2012) Chronic valproate treatment enhances postischemic angiogenesis and promotes functional recovery in a rat model of ischemic stroke. Stroke 43:2430–2436.

Wang ZF, Fessler EB, Chuang DM (2011a) Beneficial effects of mood stabilizers lithium, valproate and lamotrigine in experimental stroke models. Acta Pharmacol Sin 32:1433–1445.

Wang ZF, Leng Y, Tsai LK, Leeds P, Chuang DM (2011b) Valproic acid attenuates blood-brain barrier disruption in a rat model of transient focal cerebral ischemia: the roles of HDAC and MMP-9 inhibition. J Cerebr Blood F Met 31:52–57.

Williams MR, Hampton T, Pearce RK, Hirsch SR, Ansorge O, Thom M, Maier M (2013) Astrocyte decrease in the subgenual cingulate and callosal genu in schizophrenia. Eur Arch Psychiatry Clin Neurosci 263:41–52.

Wu XF, Chen PS, Dallas S, Wilson B, Block ML, Wang CC, Kinyamu H, Lu N, Gao X, Leng Y, Chuang DM, Zhang WQ, Lu RB, Hong JS (2008) Histone deacetylase inhibitors up-regulate astrocyte GDNF and BDNF gene transcription and protect dopaminergic neurons. Int J Neuropsychoph 11:1123–1134.

Xuan AG, Pan XB, Wei P, Ji WD, Zhang WJ, Liu JH, Hong LP, Chen WL, Long DH (2015) Valproic acid alleviates memory deficits and attenuates amyloid-beta deposition in transgenic mouse model of Alzheimer's disease. Mol Neurobiol 51:300–312.

Yaqoob U, Cao S, de Assuncao T, Shah V (2013) FGF21 promotes cirrhosis associated angiogenesis through endocytosis dependent activation of FGFR1 in endothelial cells. Hepatology 58:336a–336a.

Yaqoob U, Jagavelu K, Shergill U, de Assuncao T, Cao S, Shah VH (2014) FGF21 promotes endothelial cell angiogenesis through a dynamin-2 and Rab5 dependent pathway. Plos One 9:e98130.

Yasuda S, Liang MH, Marinova Z, Yahyavi A, Chuang DM (2009) The mood stabilizers lithium and valproate selectively activate the promoter IV of brain-derived neurotrophic factor in neurons. Mol Psychiatr 14:51–59.

Yie J, Wang W, Deng L, Tam LT, Stevens J, Chen MM, Li Y, Xu J, Lindberg R, Hecht R, Veniant M, Chen C, Wang M (2012) Understanding the physical interactions in the FGF21/FGFR/beta-Klotho complex: structural requirements and implications in FGF21 signaling. Chem Biol Drug Des 79:398–410.

Yu Y, Bai F, Wang W, Liu Y, Yuan Q, Qu S, Zhang T, Tian G, Li S, Li D, Ren G (2015) Fibroblast growth factor 21 protects mouse brain against d-galactose induced aging via suppression of oxidative stress response and advanced glycation end products formation. Pharmacol Biochem Behav 133:122–131.

Zadori D, Geisz A, Vamos E, Vecsei L, Klivenyi P (2009) Valproate ameliorates the survival and the motor performance in a transgenic mouse model of Huntington's disease. Pharmacol Biochem Behav 94:148–153.

Zhang C, Tan Y, Miao X, Bai Y, Feng WK, Li XK, Cai L (2012a) Fgf21 expresses in diabetic hearts and protects from palmitate- and diabetes-induced cardiac cell death in vitro and in vivo via Erkl/2-dependent P38 Mapk/ampk signaling pathways. Circulation 126:A16139.

Zhang Y, Xie Y, Berglund ED, Coate KC, He TT, Katafuchi T, Xiao G, Potthoff MJ, Wei W, Wan Y, Yu RT, Evans RM, Kliewer SA, Mangelsdorf DJ (2012b) The starvation hormone, fibroblast growth factor-21, extends lifespan in mice. Elife 1:e00065.

Zhao Y, Dunbar JD, Kharitonenkov A (2012) Fgf21 as a Therapeutic reagent. Adv Exp Med Biol 728:214–228.

Zhou W, Bercury K, Cummiskey J, Luong N, Lebin J, Freed CR (2011) Phenylbutyrate up-regulates the DJ-1 protein and protects neurons in cell culture and in animal models of Parkinson disease. J Biol Chem 286:14941–14951.

Zhu Y, Yu T, Zhang XC, Nagasawa T, Wu JY, Rao Y (2002) Role of the chemokine SDF-1 as the meningeal attractant for embryonic cerebellar neurons. Nat Neurosci 5:719–720.